Available online at www.sciencedirect.com
SCIENCE DIRECT®
Chemical Physics Letters 399 (2004) 260–265
CHEMICAL PHYSICS LETTERS
www.elsevier.com/locate/cplett

A regular isomerization path among chaotic vibrational states of $CH_2(\tilde{a}^1A_1)$

Stavros C. Farantos [a,b,*], Shi Ying Lin [c], Hua Guo [c]

[a] Department of Chemistry, University of Crete, Iraklion, Crete 71110, Greece
[b] Institute of Electronic Structure and Laser, FORTH, Iraklion 71110, Greece
[c] Department of Chemistry, University of New Mexico, Albuquerque, NM 87131, USA

Received 21 September 2004; in final form 5 October 2004
Available online 28 October 2004

Abstract

The nearest neighbor level spacing and Δ_3 distributions indicate that the vibrational spectrum of $CH_2(\tilde{a}^1A_1)$ is largely chaotic. Nevertheless, regular localized states coexist with the chaotic ones and they are related to overtone states of the principal vibrational modes. Periodic orbits accompanied by a stability analysis identify these states and explain their topologies and localization in configuration space. Particularly, the bending vibrational mode which is associated to the isomerization pathway which connects two equivalent minima separated by a linear symmetric saddle point, shows the dip in energy level spacings at the region of the saddle point. The corresponding wave functions are identified by periodic orbits emanated from saddle-node bifurcations below and above the barrier of isomerization.

1. Introduction

Vibrational molecular spectroscopy has seen significant advances in the last decades [1]. Methods such as Stimulated Emission Pumping, Laser Induced Fluorescence and Overtone Spectroscopy are among those used to excite molecules at high vibrational levels and record spectra close and above the isomerization or dissociation thresholds. Parallel to the experimental work new theories and algorithms have been developed to calculate hundreds of vibrational quantum energy levels and wave functions using accurate potential energy surfaces (PES). The importance of this work stems from our efforts in understanding the dynamics of the molecule close to the reaction threshold.

The PES, even for a triatomic molecule, is a complex non-linear multi-dimensional function with a landscape that has several minima and saddle points. In elementary chemical reactions specific bonds break and/or form requiring the localization of energy to specific regions of the PES. How such processes can be traced in the vibrational spectra? To answer this question usually a global molecular potential produced by ab initio electronic structure calculations is employed. Given the PES the eigenenergies and the eigenfunctions of the molecule are calculated by solving the nuclear Schrödinger equation. Although for small molecules it is feasible to examine every state separately, generally some statistical measures related to the energy difference of adjacent levels are used to distinguish regular from chaotic behaviors. Nevertheless, at high excitation energies the knowledge of the eigenenergies and eigenfunctions alone is not enough to extract the mechanisms of energy localization, and thus, the breaking/forming of a bond. Such mechanisms are better investigated in the limit of classical mechanics. Classical mechanics provide the means for a detailed analysis of the motions of non-linear systems. In Hamiltonian systems stationary phase space

* Corresponding author. Fax: +30 2810 391305.
E-mail address: farantos@iesl.forth.gr (S.C. Farantos).

0009-2614/$ - see front matter © 2004 Elsevier B.V. All rights reserved.
doi:10.1016/j.cplett.2004.10.018

structures, among which periodic orbits, tori, stable and unstable manifolds, play the protagonists role in elucidating the dynamics.

The stationary (or equilibrium) points of the potential function (minima, maxima and saddles) dictate the dynamics of molecules in the nearby energies. However, if we want to understand chemical reactions the potential function alone is not adequate. The knowledge of the geometry of phase space is required. For example, it has recently been shown, that the very important concept of the transition state, a hypersurface in phase space which reactive trajectories must cross only once, is based on the definition of the phase space structure called normally hyperbolic invariant manifold (NHIM) [2–4]. The need for phase space objects in elucidating the dynamics of the molecule at energies far from the equilibrium points becomes imperative. The molecule even before reaching the reaction (isomerization or dissociation) threshold develops complicated phase space structures when resonance conditions are satisfied among its degrees of freedom. These structures, which may be regular or chaotic, are energy dependent and they may be formed or destroyed as energy varies.

As stationary points determine the topography of the PES, periodic orbits (POs) play a similar role for the topology of phase space. They determine the dynamics of the molecule in their neighborhoods, but most importantly, at energies far from the equilibrium points. Plots of the initial conditions or/and the periods of POs with the energy consist of what we call continuation/bifurcation (C/B) diagrams [5–8]. POs and C/B diagrams enable us to establish a classical-quantum correspondence and to illustrate spectroscopic peculiarities and the topologies of the wave functions. We have applied the above scheme to several triatomic molecules and for bound and unbound energies. Via POs we follow the evolution of normal mode motions to higher energies where non-linearities are important. Bifurcations of periodic orbits mean the genesis of new POs, and thus, new type of motions.

The methylene (CH_2) molecule in its first singlet excited state, $\tilde{a}^1A_1$, has been the theme of recent quantum dynamical studies by some of us [9–11]. These studies were mainly concerned with the reactive and inelastic scattering between $C(^1D)$ and H_2. CH_2 is an important intermediate in many organic reactions, in astrochemistry as well as in combustion processes. Thus, it is not surprising that it has been the subject of extensive spectroscopic investigations [12] and theoretical calculations [13]. The purpose of the present article is to examine vibrationally bound states of the molecule excited above the linearization barrier. For symmetric collinear geometries (H–C–H) there is a saddle point which separates the two minima with C_{2v} symmetry of the molecule. We show that the overtone states are regular in spite of the overall irregular behavior extracted from the statistics in level spacing. More importantly, we demonstrate that the dip observed in level spacing of the bend overtones at energies close to the isomerization threshold is due to states which are associated with periodic orbits emanated from saddle-node bifurcations below and above the saddle-point. These results are discussed in connection to previous studies on a spherical pendulum model [14] and HCP molecule [6,15].

2. Numerical methods

A hierarchical way to extract the global dynamics of a dynamical system starts with the location of the stationary points on the PES. If we denote the generalized coordinates by $\vec{q}$ and their conjugate momenta by $\vec{p}$, the stationary points are those points in phase space which satisfy the equations $\dot{\vec{q}} = 0$ and $\dot{\vec{p}} = 0$, i.e., generalized velocities and forces are zero. The next step is to locate periodic orbits. Periodic solutions with period T of the equations of motion are found by locating those initial coordinates and momenta which satisfy the equations $\vec{q}(T) = \vec{q}(0)$ and $\vec{p}(T) = \vec{p}(0)$.

Stationary points and periodic orbits are located with the program POMULT, a package of Fortran programs which implement multiple shooting algorithms for solving two-point boundary value problems [16]. The potential energy surface for the $\tilde{a}^1A_1$-state of CH_2 has been described before [17,18]. Analytic first and second derivatives of the potential function required in the calculation of periodic orbits and their stability analysis are computed by the AUTO_DERIV, a Fortran code for automatic differentiation of any analytic function of many variables written in Fortran [19].

Following our previous practice we extract the global classical dynamics of methylene on the $\tilde{a}^1A_1$ potential by locating families of periodic orbits. We start from the minimum of the potential by finding the principal families which correspond to the normal modes of the molecule. Then, continuation methods applied with the period as a parameter [20] reveal how the stability of the periodic orbits change with energy in a specific family. Bifurcations are predicted and new families of POs are located. The C/B diagram is then compared with the quantum mechanical vibrational overtone level spacing. To investigate how the normal modes evolve from the minimum to the saddle point we find POs in an energy range which spans more than 2 eV.

The vibrational energy levels of $CH_2(J = 0)$ were determined using the recursive Lanczos algorithm [21]. The wave functions were generated by assembling the Lanczos vectors in additional recursion [22]. The reactant ($C + H_2$) Jacobi coordinates (r,R,θ) was used to take advantage of the exchange symmetry. The discretization of the Hamiltonian has been detailed in our previous work [9] and is not discussed here. The numerical parameters are summarized as follows: 188 equidistant

grid points were taken for $R \in (0,16)$ a.u., and 99 equidistant grid points for $r \in (0.5,15)$ a.u. A 35-point Gauss–Legendre quadrature DVR was used for the angular degree of freedom, which corresponds to $j_{max} = 68$. The PES and the rotational kinetic energy were truncated at 0.5 Hartree. Seventy five thousand Lanczos steps were found to be sufficient to converge all bound states with even exchange symmetry.

3. Results and discussion

A total of 602 vibrational states was found below the dissociation limit. Due to the space limitation only low-lying energy levels are listed in Table 1. The normal mode assignments are also given in the same table. The assignments were based primarily on the node structure of the corresponding eigenstates. As energy increases, the assignment becomes more difficult because of the irregularities of eigenstates and Fermi resonances. Three misassignments at 8241, 8328, and 8361 cm^{-1} reported in our earlier work [9] are corrected. To investigate the statistical behavior of the bound state spectrum, the nearest neighbor spacing distribution (NNSD) and Δ_3 distribution were computed and depicted in Fig. 1. The spectrum was first unfolded using the method of Haller et al. [23] so that the mean nearest neighbor spacing is close to unity. As the figure shows, the NNSD is close to the Wigner distribution [24], indicating that the short-range fluctuation of the vibrational spectrum is mostly chaotic. To be more quantitative, the distribution is also fitted to the Brody distribution[25], as shown in the same figure. The fitted Brody parameter of 0.64 confirms significant level repulsion in the system. The long-range Δ_3 distribution[26] also indicate the dominance of the chaotic character.

Table 1
Low-lying CH_2 vibrational levels for $J = 0$ and even symmetry

E (cm^{-1})	(v_1,v_2,v_3)	E (cm^{-1})	(v_1,v_2,v_3)
0.0	(0,0,0)	8944.11	(0,8,0)
1338.05	(0,1,0)	9112.61	(1,5,0)
2642.88	(0,2,0)	9335.60	(2,3,0)
2803.76	(1,0,0)	9476.89	(3,1,0)
3903.92	(0,3,0)	9579.31	(0,3,2)
4122.54	(1,1,0)	9660.49	(1,1,2)
5116.99	(0,4,0)	9929.59	(0,9,0)
5414.01	(1,2,0)	10144.73	(1,6,0)
5530.31	(2,0,0)	10512.15	(2,4,0)
5750.89	(0,0,2)	10628.63	(4,0,0)
6271.16	(0,5,0)	10746.48	(3,2,0)
6663.19	(1,3,0)	10783.76	(0,4,2)
6847.48	(2,1,0)	10871.44	(1,2,2)
7052.02	(0,1,2)	10908.99	(1,7,0)
7333.04	(0,6,0)	10961.77	(2,1,2)
7857.92	(1,4,0)	11143.00	(0,10,0)
8094.74	(2,2,0)	11189.04	(0,0,4)
8176.25	(3,0,0)	11584.63	(1,8,0)
8241.72	(0,7,0)	11786.95	(2,5,0)
8328.78	(0,2,2)	11884.94	(4,1,0)
8361.41	(1,0,2)	11951.04	(0,5,2)

The assignment is given in normal mode quantum numbers (v_1,v_2,v_3) for symmetric stretch, bend, and anti-symmetric stretch modes, respectively.

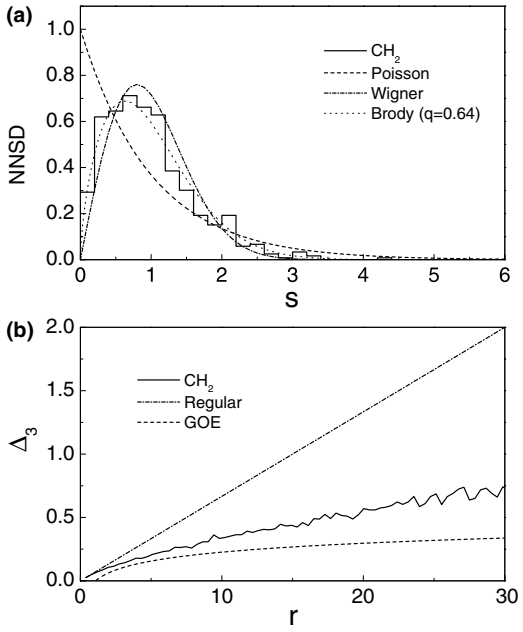

Fig. 1. Nearest neighbor spacing distribution (a) and Δ_3 distribution (b) of CH_2 bound states for $J = 0$ and even exchange symmetry. The Poisson and Wigner distributions represent the regular and chaotic limits for the NNSD. For the Δ_3 distribution, the chaotic limit is given by the Gaussian Orthogonal Ensemble (GOE).

As the figure shows the NNSD is close to the Wigner distribution[24], indicating that the short-range fluctuation of the vibrational spectrum is mostly chaotic. The long range Δ_3 distribution [26] also indicates the dominance of the chaotic character.

The potential has two equivalent minima of C_{2v} symmetry separated by a linear saddle point (1.095 eV). From each minimum a number of families of stable periodic orbits emanate at least as many as the number of normal modes the motions of which represent [27]. For saddle points the principal periodic orbits are unstable [28]. A projection of the continuation/bifurcation diagram of POs is to plot the frequencies ($\omega = 2\pi/T$) of the periodic orbits as functions of the total energy. Such a C/B diagram is shown in Fig. 2.

The continuous lines denote the frequencies of periodic orbits as functions of the total energy E. A3 is the family that corresponds to the bend normal mode, A2 to the symmetric stretch and A1 to the asymmetric stretch mode. The harmonic frequencies are estimated to be $\omega_1 = 3069$ cm^{-1} for the asymmetric stretch, and $\omega_2 = 2906$ cm^{-1} for the symmetric stretch, and $\omega_3 = 1382$ cm^{-1} for the bend. Note that the A2

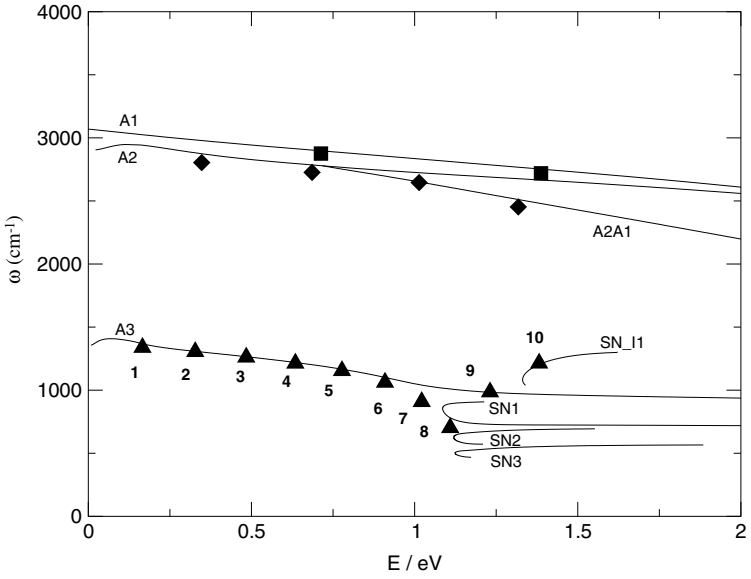

Fig. 2. Periodic orbit continuation/bifurcation diagram of the $\tilde{a}^1A_1$-state of CH_2. A3 is the family that corresponds to the bend normal mode, A2 to the symmetric stretch and A1 to the asymmetric stretch mode. The symbols represent the energy spacings between neighboring quantum states of the overtone progressions; squares for the anti-symmetric stretch, diamonds for the symmetric stretch and triangles for the bend. SN denotes periodic orbits emanated from saddle-node bifurcations. Note, that the even quantum number states for the anti-symmetric stretch are shown ($v_3 = 2,4$).

and A3 families show a negative anharmonicity (frequencies increase) very close to the minimum of the potential. It is difficult to say whether this is an artifact of the potential function or a genuine behavior of methylene. The continuation lines in Fig. 2 do not distinguish stable from unstable POs. The A1 family remains stable for the energy range shown but the A2 symmetric stretch family becomes early single unstable and after its bifurcation at about 0.7 eV double unstable. The bifurcating A2A1 family is initially single unstable but it becomes stable at energies above the saddle point. The A3 is stable up to the barrier of isomerization after which it becomes single and later double unstable. We may conclude that extended chaos sets in at energies above the linearization barrier.

As we have shown in our previous studies [5–8] the Hamiltonian saddle-node (SN) bifurcation is the most common elementary bifurcation [29] found in molecular systems. Their importance is due to the creation of new periodic orbits suddenly at some critical energy with stable motions embedded in chaotic regions. That causes the localization of energy, a significant effect in chemical dynamics. A cascade of such SN bifurcations appear as we approach the saddle point of the linearized molecule. This scenario, seen also previously, is typical as the parent family approaches the bifurcation critical energy. Its frequency levels off and two new families appear with one branch showing high anharmonicity. As energy increases the frequency of the daughter most anharmonic family starts leveling off again and a new SN bifurcation takes place. The mechanism of generating this cascade of saddle-node bifurcations can be understood as a cascade of resonances between coupled oscillators [30].

Representative periodic orbits are shown in Fig. 3 projected in the (R,r) Jacobi coordinate plane and overlayed on the potential contours. The A1 PO has mainly excitation along the angle Jacobi coordinate. The energies of these periodic orbits are above the barrier of linearization. The SN_I1 represents periodic orbits which surpass the barrier of isomerization. These POs also originate from a saddle-node bifurcation and as we describe it later on they mark isomerizing quantum states.

The classical frequencies are compared with the energy difference between adjacent quantum eigenenergies for the three series of overtone vibrational progressions. We have not tried to semiclassically quantize accurately the periodic orbits [31]. In a rather simple approach we compare classical and quantum mechanical eigenfrequencies, by shifting the quantum energies by the zero-point-energy and we plot the energy differences with respect to the upper level. As we can see, the anharmonicity of the overtone states closely follows that of the frequencies of the periodic orbits. The good correspondence among POs and eigenfunctions is better demonstrated in a pictorial way in Fig. 4.

We see that in spite of the irregular behavior predicted by the statistical measures for $CH_2(\tilde{a}^1A_1)$, the overtone states of the bending mode are regular and well localized in configuration space up to and above the barrier to linearization. This was one of the conclusions of Green et al. [13]. These investigators carried out an extensive ab initio study of the two lowest singlet excited states of methylene, $\tilde{a}^1A_1$ and $\tilde{b}^1B_1$, which are degenerate for linear geometries and they are separated for planar geometries because of the Renner–Teller interaction. Since this work takes in account the Renner–Teller

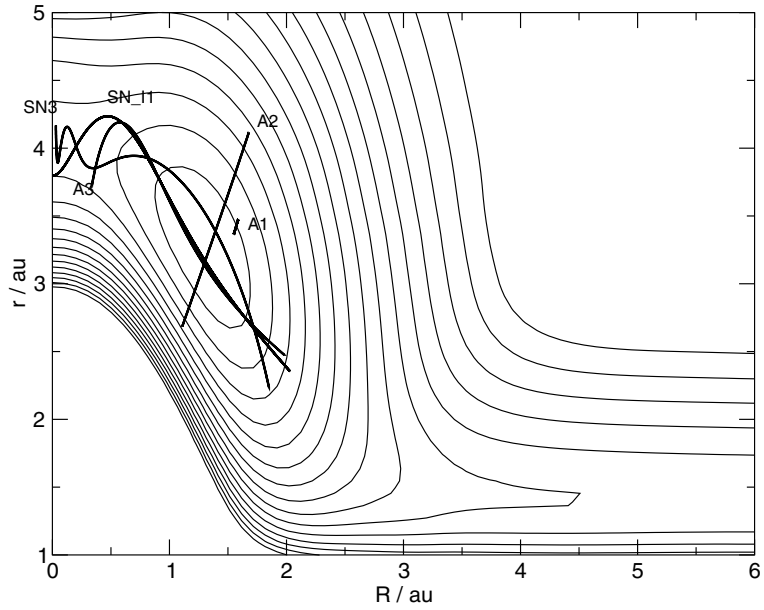

Fig. 3. Representative periodic orbits from each family of POs shown in Fig. 2, and projected onto the (R,r)-plane together with contours of the PES.

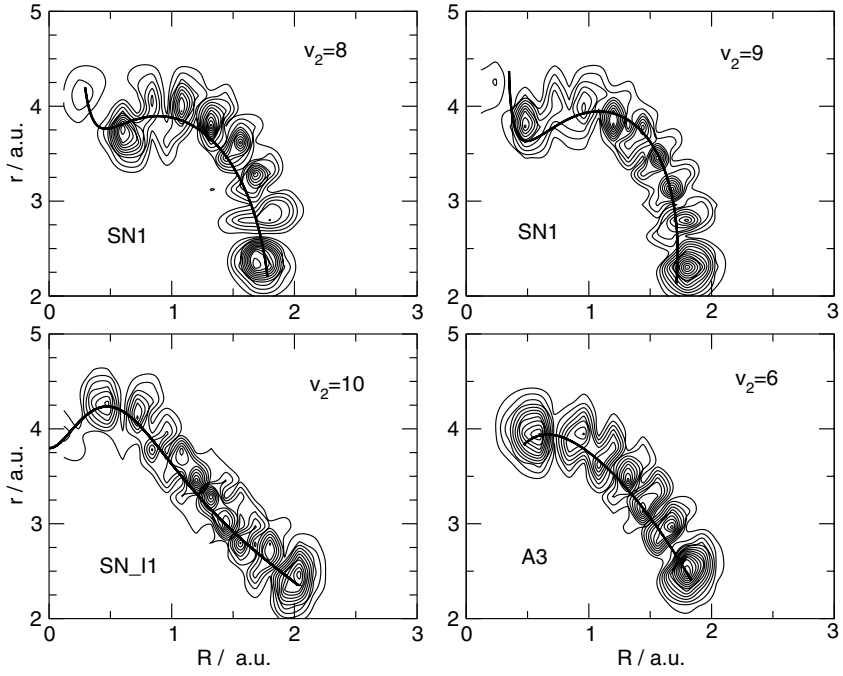

Fig. 4. Regular localized wave functions of the bend mode marked by periodic orbits at approximately the same energy.

interaction in the rotation–vibration calculations and it concludes as us, we may infer that there is no strong interaction between the two surfaces.

It turns out, that the cascade of saddle-node bifurcations of periodic orbits is a generic mechanism to approach isomerization or dissociation thresholds as previous studies in triatomic molecules have revealed [6–8]. The stable or the least unstable branches of these bifurcations trace the most stable regions in phase space where the quantum mechanical eigenfunctions are localized. Spectroscopic evidence for such states, also named saddle-node, have been found for HCP [6]. The spectroscopic characteristic of this molecule is a 2:1 Fermi resonance between the CP stretch and bend. Jacobson and Child [14,15] studied a spherical pendulum model Hamiltonian of the Fermi resonance and found the

dip in the energy level spacing, which is a characteristic of the saddle point. However, as the authors point out one must be aware of the differences in the above the barrier states for molecules which mimic a spherical pendulum model, like HCP, and Renner–Teller systems like the one studied in this article. Although spectroscopic differences for these two molecules, HCP and CH_2, are expected, the classical interpretation by periodic orbits is the same; the quantum states are associated to saddle-node bifurcations. Above the barrier the SN periodic orbits are those which connect the two minima and they have been named isomerizing.

An interesting question is whether SN bifurcations below and above the barrier have the same origin. Those which are born below the barrier may be thought of as the result of the rapid change in the anharmonicity along the reaction path which brings the system in multiple resonances as energy varies. On the other hand, those above the barrier are associated with the unstable periodic orbits originated from the saddle point and the Newhouse wild hyperbolic set [32,5,33]. Obviously, more studies are need to answer this question.

Acknowledgements

We are thankful to Dr. Reinhard Schinke for his remarks. This work at UNM was supported by the National Science Foundation (CHE-0348858). Support from the Greek Ministry of Education and European Union through the postgraduate program EPEAEK, 'Applied Molecular Spectroscopy', is gratefully acknowledged.

References

[1] H.-L. Dai, R.W. Field, Molecular Dynamics and Spectroscopy by Stimulated Emission Pumping, in: Advanced Series in Physical Chemistry, vol. 4, World Scientific, Singapore, 1995.
[2] S. Wiggins, Normally Hyperbolic Invariant Manifolds in Dynamical Systems, Springer, 1994.
[3] T. Uzer, C. Jaffé, J. Palacián, P. Yanguas, S. Wiggins, Nonlinearity 15 (2002) 957.
[4] H. Waalkens, A. Burbanks, S. Wiggins, J. Chem. Phys., (2004) in press.
[5] S.C. Farantos, Int. Rev. Phys. Chem. 15 (1996) 345.
[6] H. Ishikawa, R.W. Field, S.C. Farantos, M. Joyeux, J. Koput, C. Beck, R. Schinke, Annu. Rev. Phys. Chem. 50 (1999) 443.
[7] M. Joyeux, S.C. Farantos, R. Schinke, J. Phys. Chem. 106 (2002) 5407.
[8] M. Joyeux, S. Yu. Grebenshchikov, J. Bredenbeck, R. Schinke, S.C. Farantos, Adv. Chem. Phys., in press (2005).
[9] S.Y. Lin, H. Guo, J. Chem. Phys. 119 (2003) 11602.
[10] S.Y. Lin, H. Guo, J. Phys. Chem. A 108 (2004) 2141.
[11] S.Y. Lin, H. Guo, J. Chem. Phys. 121 (2004) 1285; S.Y. Lin, H. Guo, J. Chem. Phys. 120 (2004) 9907.
[12] G.V. Hartland, D. Qin, H.-L. Dai, J. Chem. Phys. 102 (1995) 6641.
[13] W.H. Green Jr., N.C. Handy, P.J. Knowles, S. Carter, J. Chem. Phys. 94 (1991) 118.
[14] M.P. Jacobson, M.S. Child, J. Chem. Phys. 114 (2001) 250.
[15] M.P. Jacobson, M.S. Child, J. Chem. Phys. 114 (2001) 262.
[16] S.C. Farantos, Comput. Phys. Commun. 108 (1998) 240.
[17] L. Bañares, F.J. Aoiz, S.A. Vázquez, T.-S. Ho, H. Rabitz, Chem. Phys. Lett. 374 (2003) 243.
[18] B. Bussery-Honvault, P. Honvault, J.-M. Launay, J. Chem. Phys. 115 (2001) 10701.
[19] S. Stamatiadis, R. Prosmiti, S.C. Farantos, Comput. Phys. Commun. 127 (2000) 343.
[20] E.L. Allgower, K. Georg, Numerical Continuation Methods, Springer Series in Computational Mathematics, vol. 13, Springer, Berlin, 1993.
[21] C. Lanczos, J. Res. Natl. Bur. Stand. 45 (1950) 255.
[22] J.K. Cullum, R.A. Willoughby, Lanczos Algorithms for Large Symmetric Eigenvalue Computations, Birkhauser, Boston, 1985.
[23] E. Haller, H. Koppel, L.S. Cederbaum, Chem. Phys. Lett. 101 (1983) 215.
[24] E.P. Wigner, SIAM Rev. 1 (1967) 1.
[25] T.A. Brody, J. Flores, J.B. French, P.A. Mello, A. Pandey, S.S.M. Wong, Rev. Mod. Phys. 53 (1981) 385.
[26] F.J. Dyson, M.L. Mehta, J. Math. Phys. 4 (1963) 701.
[27] A. Weinstein, Inv. Math. 20 (1973) 47.
[28] J. Moser, Commun. Pure Appl. Math. 29 (1976) 727.
[29] S. Wiggins, Introduction to Applied Nonlinear Dynamical Systems and Chaos, second edn., vol. 2, Springer, New York, 2003.
[30] G. Kopidakis, S. Aubry, Physica D 130 (1999) 155.
[31] M.C. Gutzwiller, Chaos in Classical and Quantum Mechanics, vol. 1, Springer, 1990.
[32] S.E. Newhouse, Publ. Math. IHES 50 (1979) 101.
[33] F. Borondo, A.A. Zembekov, R.M. Benito, J. Chem. Phys. 105 (1996) 5068.